JOURNAL OF SPACECRAFT AND ROCKETS
Vol. 43, No. 2, March–April 2006

Homogeneous Silica Formed by the Oxidation of Si(100) in Hyperthermal Atomic Oxygen

Maja Kisa,* Long Li,† and Judith Yang‡
University of Pittsburgh, Pittsburgh, Pennsylvania 15261
Timothy K. Minton§
Montana State University, Bozeman, Montana 59717
William G. Stratton* and Paul Voyles¶
University of Wisconsin–Madison, Madison, Wisconsin 53706
Xidong Chen**
Cedarville University, Cedarville, Ohio 45314
and
Klaus van Benthem†† and Steve J. Pennycook‡‡
Oak Ridge National Laboratory, Oak Ridge, Tennessee 37831

We review and summarize all of our microstructural comparisons of the silica and Si/SiO_x interface created by the oxidation of Si(100) in atomic oxygen and molecular oxygen, using primarily electron microscopy techniques. A laser detonation source was used to produce atomic oxygen with kinetic energy 5.1 eV, whereas a conventional furnace was used to expose Si single crystal to thermal molecular oxygen. The silica formed on Si(100) by atomic oxygen is thicker, more homogeneous, and less amorphous (similar to alpha-quartz), as compared to the oxide layer created by molecular oxygen. High-angle annular dark field imaging and high-spatial-resolution electron energy loss spectroscopy confirmed that the Si/SiO_x interface created by atomic oxygen is abrupt, containing no suboxides, as opposed to the broad interface with transitional states formed by molecular oxygen. Preliminary fluctuation electron microscopy results confirmed increased medium-range ordering in SiO_x formed by atomic oxygen compared to the nonregular arrangement present in the amorphous oxide formed by the oxidation of Si(100) in molecular oxygen. Differences in the oxide films grown by exposure to atomic and molecular oxygen are discussed in the context of the thermionic emission model of silicon oxidation.

I. Introduction

ATOMIC oxygen (AO) is the most corrosive element in low earth orbit (LEO), causing rapid degradation of spacecraft materials exposed to this harsh environment. Spacecraft that travel through the residual atmosphere at LEO altitudes (200–700 km) have velocities of ~7.8 km s^{-1} and undergo impacts with atomic oxygen that are equivalent to O atoms with ~4.5 eV of translational energy striking the leading edge (or ram surface) of the spacecraft.[1] The flux of these energetic O-atom collisions may be $\sim 10^{15}$ O atoms cm^{-2} s^{-1}. Polymers are the materials that erode most rapidly in the LEO environment. Thin films of metals, such as Al, or semiconductor oxides, such as silica, can protect polymer materials and limit their erosion rate. Current approaches to protecting polymers from erosion in LEO include coating the polymer with SiO_x ($1.9 \leq x \leq 2.0$) (Refs. 2 and 3) or incorporating Si into a polymer structure so that a passivating SiO_x layer will be formed upon atomic-oxygen exposure.[4] Adhesion to the polymer, uniformity of the coating, and small number of imperfections, such as pinholes, are desired qualities for the coatings.[5,6] Characterizing the microstructure of these coatings, including film thickness and uniformity, is needed to elucidate the pathways through which atomic oxygen can penetrate and cause undercutting of the underlying polymer.

In this paper, we review our results on the oxide thickness and the Si/SiO_x interface formed by the exposure of Si(100) samples to atomic oxygen as well as our recent investigations of the amorphous structure of the oxide film. This study illustrates the striking differences in the chemistry and structure of the oxide films when they are formed on Si(100) surfaces by different reagent oxygen species at relatively low temperatures. We suggest that differences in the oxide films are due, in part, to enhanced thermionic emission of electrons when the surface is bombarded by energetic oxygen atoms.

II. Experimental

Boron-doped single-crystal silicon wafers, double-side polished, with a resistivity of 10–50 Ω cm, and average surface roughness of 1 nm were obtained from MTI Corporation.[7] The silicon samples were cleaned with the use of an HF dip before exposure to atomic oxygen.[8–12] Before oxidation by molecular oxygen, the samples were cleaned using a Radio Corp. of America (RCA) cleaning procedure.[13] In both HF and RCA cleaning procedures, rinsing in deionized water was performed to remove organics and residual fluorine on the silicon surface. After cleaning, the samples were immediately mounted in a vacuum chamber for atomic oxygen exposure or placed inside a furnace for molecular oxygen exposure. A laser detonation source, based on the breakdown of oxygen gas by a CO_2 transversely excited atmosphere (TEA) laser pulsed at 2 Hz, was utilized to produce atomic oxygen with 5.1 eV kinetic energy.[14–16] The beam contained atomic and molecular oxygen in a ratio of 70:30. The nominal translational energy of the atomic oxygen in the beam was 5.1 eV. The silicon samples were mounted on a temperature-controlled sample holder that was held at 493 K during exposure to the beam. The orientation of the samples was such

Received 22 April 2005; accepted for publication 25 August 2005.

*Graduate Student, Materials Science and Engineering Department.
†Research Associate, Materials Science and Engineering Department.
‡Associate Professor, Materials Science and Engineering Department.
§Associate Professor, Department of Chemistry and Biochemistry.
¶Assistant Professor, Materials Science and Engineering Department.
**Assistant Professor, Department of Science and Mathematics.
††Postdoctoral Fellow, Solid State Division.
‡‡Research Staff, Solid State Division.

that the angle of incidence of the beam was within a few degrees of the surface normal. Four samples were exposed in the reaction chamber for 50,000 beam pulses, which corresponds to an atomic oxygen fluence of 8×10^{19} atoms cm^{-2}, as verified by the use of a Kapton witness sample. After exposure to the AO beam, the samples were allowed to cool to room temperature in the vacuum chamber. Oxidation with molecular oxygen was performed in a conventional clamshell one-zone Leybold furnace with a mulite tube controlled by a Eurotherm proportional integral derivative (PID) controller. The temperature was ramped to 493 K, and the oxygen pressure was set to 1 atm. The exposure period of 48 h produced a completely passivating silica layer that did not change upon further exposure to air.

The microstructure of the silica film and the oxide/metal interface was characterized with high-resolution transmission electron microscopy (HRTEM), electron energy loss spectroscopy (EELS), and selected area electron diffraction (SAED) in a JEM 2010F electron microscope operated at 200 keV with a spatial resolution of 0.18 nm. High-angle annular dark-field (HAADF) imaging and high-spatial-resolution EELS data were acquired with a parallel electron energy loss spectrometer attached to an aberration-corrected VG HB501 dedicated scanning transmission electron microscope (STEM), operating at 100 kV. This microscope is capable of achieving an energy resolution better than 0.5 eV, with a spatial resolution below 0.1 nm. The methods used for the preparation of cross-sectional and plan-view TEM samples are described elsewhere.[16] Radial distribution function (RDF) analyses and fluctuation electron microscopy (FEM) were also used to characterize the amorphous oxide.[17] An RDF analysis was performed on the SAED patterns of the oxide using Gatan Digital Micrograph script. FEM data were taken on a LEO 912 EFTEM, operating at 120 kV, with 16-Å spatial resolution.

III. Results

The silica formed on Si(100) exposed to atomic oxygen is almost two times thicker than the oxide formed on Si(100) oxidized in molecular oxygen.[16] Figure 1 shows cross-sectional HRTEM micrographs of the silicon oxide layers formed by atomic oxygen (Fig. 1a) and molecular oxygen (Fig. 1b). The Si$L_{2,3}$ spectrum images across the Si/silica interface, taken from aberration-corrected STEM with atomic-level spatial resolution, are shown in Fig. 2b. Only Si^0 (99.8 eV), in the Si, and Si^{4+} (103.5 eV) oxidation states, in the oxide, were detected, where no additional peaks are noted near the interface, or in the oxide, that would indicate the presence of suboxide states. From a comparison with the results of Garvie et al. on the various Si$L_{2,3}$ edges for various phases of silica, the oxide formed by AO is most similar to that of alpha-quartz, as opposed to the amorphous silica created by molecular oxygen.[18,19]

SAED patterns of Si(100) oxidized by atomic and molecular oxygen species are shown in Figs. 3a and 3b. The SAED pattern of the Si(100) oxidized by molecular oxygen (Fig. 3b) showed diffused halo rings, characteristic of amorphous materials. Sharper diffraction rings are present in the diffraction pattern of Si(100) oxidized by hyperthermal atomic oxygen (Fig. 3a), where the diffraction rings were identified as polycrystalline alpha-quartz. The observed lattice spacings for the oxide created by reactive atomic oxygen, namely $d_{200} = 2.070$ Å, $d_{112} = 1.783$ Å, $d_{014} = 1.282$ Å, and $d_{033} = 1.085$ Å, correspond to those of alpha-quartz. The lattice parameters for the oxide created by atomic oxygen were determined to be $a = 4.78 \pm 0.1$ and $c = 5.13 \pm 0.1$ Å, whereas they were $a = 4.9134$ and $c = 5.4052$ Å for alpha-quartz. Experimental lattice parameters are smaller than those of alpha-quartz, suggesting that the silica layer created by atomic oxygen is under compression.[20,21]

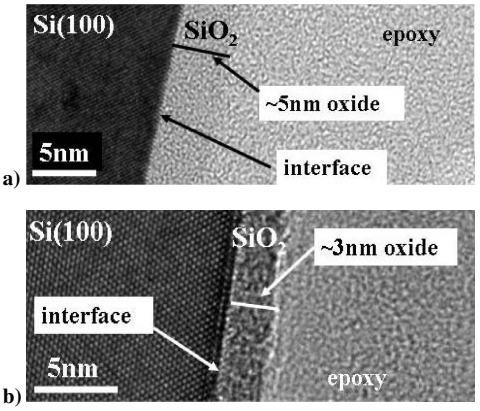

Fig. 1 HRTEM micrograph acquired on JEM 2010F microscope of cross-sectional TEM sample of Si(100) oxidized by a) atomic oxygen and b) molecular oxygen.

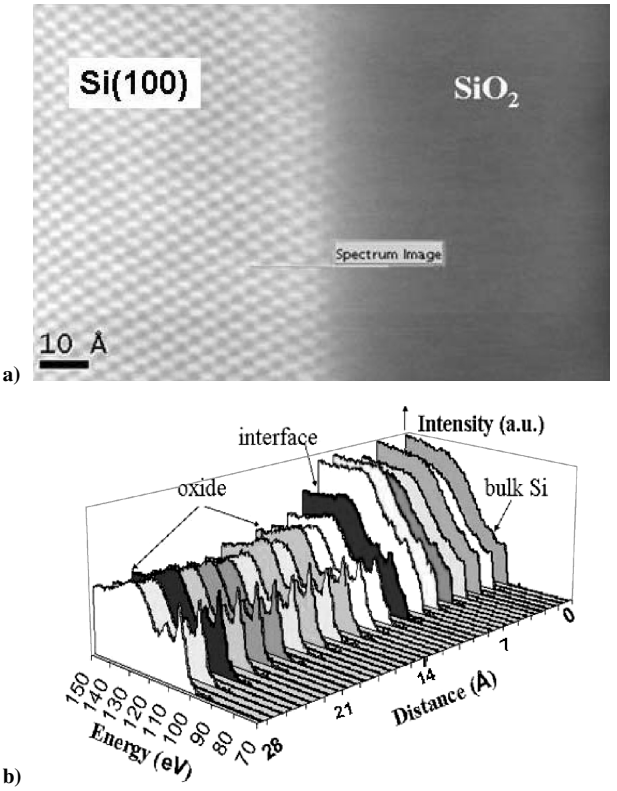

Fig. 2 Abrupt Si/SiO_2 interface formed on Si(100) oxidized by atomic oxygen: a) HAADF image of cross-sectional TEM sample ([110] zone axis) and b) background-subtracted Si$L_{2,3}$ EELS spectrum acquired on aberration-corrected VG HB501 STEM.

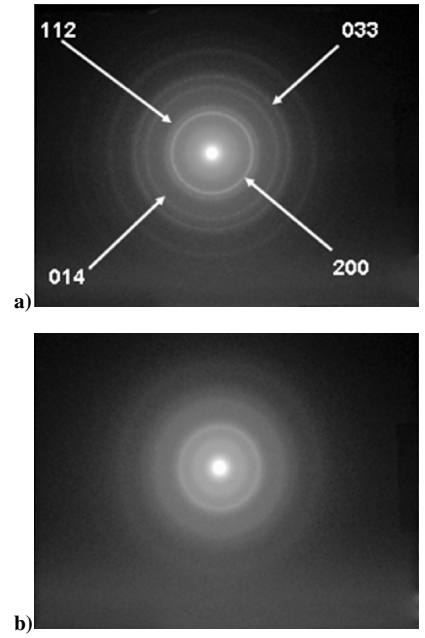

Fig. 3 SAED pattern of Si(100) oxidized by a) atomic oxygen and b) molecular oxygen.

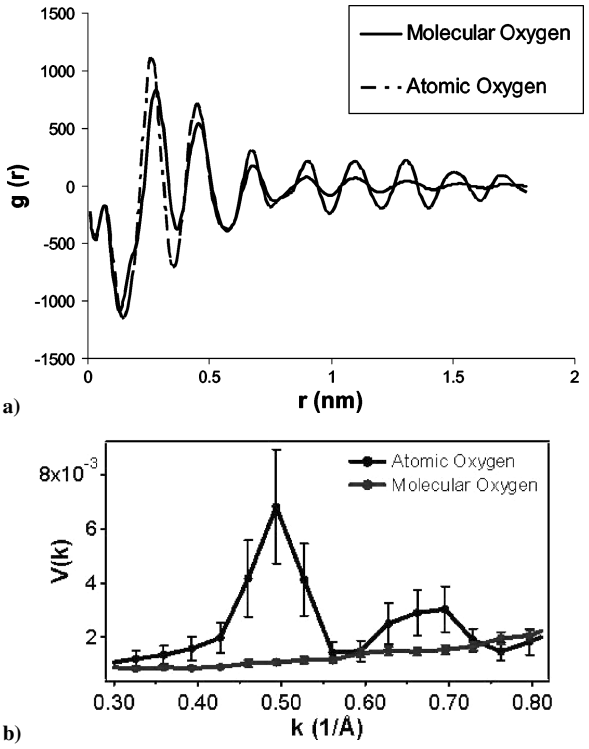

Fig. 4 Enhanced ordering in the silica formed by oxidation of Si(100) in atomic as compared to molecular oxygen: a) reduced RDF plots (short-range order) and b) variance V(k) plots (medium-range order).

This conclusion is in agreement with the previous Fourier transform infrared spectroscopy results of Tagawa et al., which revealed Si–O–Si bond angles in the oxide film created by atomic oxygen smaller than those of alpha-quartz, indicating that the SiO_2 film is under compression.[22]

A further analysis of SAED patterns is done by calculating radial distribution functions.[23] The reduced RDF's, obtained directly by Fourier transformation of experimental data, are shown in Fig. 4a. These functions oscillate about zero because the average density background r_2 dependency of the radial distribution function has been removed.[23] The peaks in the reduced RDF for the sample oxidized by atomic oxygen are more intense than those for the molecular-oxygen-oxidized sample. The reduced RDF for the atomic-oxygen-oxidized sample shows more pronounced peaks at larger r and suggests that the oxide formed by atomic oxygen is more ordered than that created by molecular oxygen. The RDF corresponds to the average of the short-range order (SRO) and cannot be used to obtain information on the medium-range order (MRO), characteristic for larger length scales.[23] Therefore, we employed variable-coherence FEM to obtain a variance curve for both samples, as shown in Fig. 4b.[17,24] An average of 10 data sets from different areas of the sample is used to obtain the variance curve, with the error bars representing the standard deviation from the mean. The positions of the peaks correspond to the internal structure or type of MRO, whereas the intensity of the peaks reflects the degree of MRO order in the material.[25] The type of MRO (peak location) and degree of MRO (peak magnitude) for Si(100) oxidized by atomic oxygen is dramatically different from that oxidized in molecular oxygen. The variance curve for the atomic-oxygen-oxidized sample shows two distinct peak locations (type of MRO) with a higher magnitude (degree of MRO) compared to any feature in the curve for the molecular-oxygen-oxidized sample, demonstrating that the atomic-oxygen-formed silica, though amorphous, has a more ordered arrangement of Si and O atoms than the molecular-oxygen-formed oxide.

IV. Discussion

The silicon oxide created by atomic oxygen on Si(100) had an average thickness of 5 nm, whereas the oxide layer formed by molecular oxygen was only 3 nm thick.[16] The increased oxide thickness due to atomic oxygen species was also observed by Tagawa et al., who examined the kinetics of oxide film growth by hyperthermal atomic oxygen on Si(100) by x-ray photoelectron spectroscopy (XPS).[26] These investigators reported the formation of a 1.75-nm-thick oxide layer, with a sample temperature of 493 K and fluence of $\sim 7 \times 10^{17}$ O atoms cm^{-2}. The nominal kinetic energy of the O atoms used was 4.6 eV. The reason that the thickness of the oxide reported by Tagawa et al. is less than half of the silica thickness that we observed may be related to the fluence, which was 100 times lower in the Tagawa experiment than in ours; hence, the oxide may not have reached its saturation thickness. We also suggested that the slightly higher kinetic energy of the atomic oxygen used in our experiments (5.1 vs 4.6 eV) may lead to a slightly thicker oxide.[21] Tagawa et al. also reported the formation of a 4.5-nm oxide scale on a sample held at 298 K following exposure of Si(100) to 5-eV atomic oxygen with a fluence of 1×10^{19} O atoms cm^{-2} (Refs. 13 and 22). The kinetic energy and fluence were comparable to our experimental conditions, but the oxidation temperature was lower, which could explain the slightly thicker oxide observed in our experiment.

The nature of the oxidizing species can affect many parameters that will alter oxidation kinetics, including structure, defects, and stress. The thermionic emission model, proposed by Irene, assumes that the rate-limiting step is the emission of electrons from Si to SiO_2.[27,28] Electrons can traverse the oxide film either by thermionic emission from the substrate to the conduction levels of the oxide or by tunneling through the oxide. Consequently, an electric potential is established between the substrate and oxygen adsorbed on the oxide surface, which causes the ions to diffuse across the oxide to form new oxide. In the case of silicon, oxygen ions diffuse inward to the Si substrate to create new silica. The primary effect of hyperthermal atomic oxygen could be increasing the number of electrons available to chemisorb the oxygen via thermionic emission.[21] Thermionic emission of electrons is not easy at low substrate temperatures. However, the high kinetic energy ($\sim$5 eV) of the atomic oxygen could provide local heating of the silicon, which would increase the number of charge carriers by enabling the electrons to overcome the energy barrier and consequently continue the oxidation reaction. Hence, as the kinetic energy increases, the limiting thickness should increase as well. Tagawa et al. showed that the limiting thickness of the silica layer increases with the kinetic energy of atomic oxygen, thus supporting our speculation that 5-eV atomic oxygen could enhance the thermionic electron flux and consequently lead to the observed increase in the oxide layer thickness.[26]

HAADF results confirm the Si/SiO_x interface abruptness for the Si(100) surface oxidized in atomic oxygen. Previous investigators demonstrated that the Si/SiO_x interface produced in ozone is also abrupt.[29,30] Itoh et al. noted that a smooth interface remained after they etched off the oxide created by ozone, and the measured the root-mean-square surface roughness, by scanning tunneling microscopy, was found to be less than 0.2 nm.[30] Uchiyama and Tsukada[31] and Itoh et al.[30] discovered that adsorption of ozone was not affected by the defect sites which are favorable locations for the initial adsorption of oxygen molecules. Hence, we further propose that atomic oxygen can be inserted directly into the back bonds, leading to the observed abrupt interface. The initial steps for the Si(100) oxidation by molecular oxygen are given on the left-hand side of Fig. 5, as originally proposed by Watanabe et al.[32] The first layer back bonds are available via O migration through the metastable surface state that provides the energy (2.96 eV for the top site, position 1, or 5.99 eV for the bridge site, position 2) for the O atom to insert itself into the Si back bonds (position 3, 4, 5, or 6), whereas direct O insertion into first- or second-layer back bond positions 5 or 6 requires energies of 1.0 or 2.4 eV, respectively. The possible steps for the Si(100) oxidation by atomic oxygen are represented on the right-hand side in Fig. 3. The atomic oxygen has 5.1-eV energy (with no bonds that need to be broken), so it can directly attack back bonds in the first and even second subsurface layer of Si. Three monolayers can thus be oxidized by atomic oxygen in the initial step, instead of only one by molecular oxygen. Hence, the initial

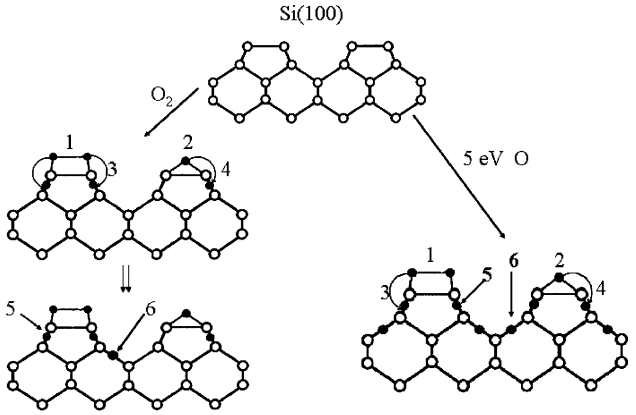

Fig. 5 Comparison of the initial steps of Si(100) surface oxidation by atomic and molecular oxygen.

rate of oxidation would be increased, resulting in an abrupt interface, with fewer transitional states for atomic oxygen as compared to molecular oxygen.

The interface abruptness and suppression of suboxide states could be explained by the ability of energetic atomic oxygen atoms to attack uppermost and first and second back bond layers.[21,32] Three monolayers can thus be oxidized by atomic oxygen in the initial step, instead of only one by molecular oxygen. Therefore, the initial rate of oxidation would be increased, resulting in an abrupt interface, with fewer transitional states for atomic oxygen as compared to molecular oxygen. Typically, interfacial abruptness may worsen the interfacial adhesion, but no differences in the interfacial adhesion or spallation were noted either after the oxidation or due to cross-sectional TEM sample preparation, indicating a reasonably adherent scale.

High-spatial-resolution EELS results confirmed previous XPS measurements of the presence of only Si^0 and Si^{4+} valence states for the Si(100) surface oxidized in atomic oxygen.[16,21] Tagawa et al. reported that the oxide scale formed by 5-eV O atoms on a room-temperature sample consisted mainly of Si^{+4} with only 6% suboxides, based on an analysis of XPS spectra.[22] The presence of only the Si^{4+} valence state for Si(100) oxidized by ozone was noted by Ichimura et al., who used XPS, second harmonic generation, and medium ion-scattering spectroscopy.[29] These EELS line spectra revealed the nanoscale uniformity of the oxide formed by atomic oxygen, showing that the Si oxidation state does not change from the Si/SiO_2 interface to the oxide surface, because no change in the position or shape of the $SiL_{2,3}$ edge was noted.

The lattice parameters determined from SAED patterns for the oxide created by atomic oxygen were found to be close to those of alpha-quartz. Tagawa et al. reported smaller Si–O–Si bond angles in the oxide film created by atomic oxygen, as compared to those of alpha-quartz, indicating that the SiO_2 film is under compression.[22] The electron loss near edge fine structures of $SiL_{2,3}$ edges also supports the finding that the oxide formed by atomic oxygen is similar to alpha-quartz. These spectra were carefully compared with the results of Garvie and Buseck for various forms of silica, including alpha-quartz, amorphous quartz (electron beam damaged quartz), opal A (SiO_2–nH_2O), and SiO_2 glass.[19] This comparison suggests that the oxidation of Si(100) by hyperthermal atomic oxygen produces a more ordered silica structure, similar to that of alpha-quartz, whereas Si(100) oxidized by molecular oxygen forms an amorphous oxide. A high energy of reactive atomic oxygen can account for the formation of more thermodynamically stable structures. The SiO_x formed by atomic oxygen is found to be more ordered and more homogeneous than silica formed in molecular oxygen, as determined by RDF. This result is in good agreement with results of Ichimura et al.,[29] who concluded that the oxide produced by ozone has an almost homogeneous structure, as implied by the constant etching rate through the oxide layer using HF. In their study of the oxidation of a different substrate, Kuznetsova et al. noted that ozone-passivated Al formed a denser and more ordered alumina as compared to molecular-oxygen-passivated Al.[33] FEM was used to further understand the differences in the structure of the oxides formed by atomic and molecular oxygen. Si(100) oxidized in atomic oxygen showed more pronounced features in the variance curve, indicating a higher degree and different type of medium-range order (MRO). The increased ordering of SiO_x due to atomic oxygen was expected, because the high energy of the oxidizing species can contribute to the formation of a more thermodynamically favorable silica structure.

V. Conclusions

The microstructure of the oxide and Si/SiO_x interface formed on Si(100) at 493 K by 5.1-eV hyperthermal atomic oxygen and thermal molecular oxygen were compared by a variety of experimental techniques including HRTEM, SAED, high-spatial-resolution EELS, HAADF, RDF, and FEM. The continual production of available electrons due to thermionic emission, facilitated by the 5.1 eV of O-atom kinetic energy, may enhance the oxidation rate of Si(100), leading to enhanced growth and thicker oxide as compared to the growth kinetics for molecular oxygen, indicating that the thickness of the silica can be controlled by the kinetic energy of the incoming oxygen species. The Si/SiO_x interface abruptness due to atomic oxygen was confirmed at the atomic level by HAADF technique. The presence of only Si^0 and Si^{4+} oxidation states across the Si/SiO_x interface formed by atomic oxygen was confirmed with high-spatial-resolution EELS. The ability for hyperthermal atomic oxygen to attack equally the uppermost, first, and second backbond layers in silicon could explain the initial increased linear oxide kinetics, homogeneity of the oxide, and interface abruptness with no detected presence of suboxides near the interface. RDF analyses and FEM results suggest that the oxide produced by 5-eV atomic oxygen has a more ordered arrangement of O and Si atoms than the silica created by molecular oxygen.

Acknowledgments

This research was funded through a multidisciplinary university research initiative sponsored by the Air Force Office of Scientific Research. The specimens were oxidized at Montana State University and at the Materials Science and Engineering Department at the University of Pittsburgh. The RBS, XPS, HRTEM, and EELS were performed at the Materials Research Laboratory, University of Illinois at Urbana–Champaign, supported by the U.S. Department of Energy. HAADF and high-resolution EELS were performed at Oak Ridge National Lab. FEM was performed at the University of Wisconsin, Madison, supported by NSF DMR 0347746. Radial distribution function was performed at Cedarville University and Argonne National Laboratory. K.v.B acknowledges funding from the Alexander von Humboldt Foundation. The assistance of R. Twesten, R. Averback, M. Williams, and R. Haach (University of Illinois) and F. Xu, J. Barnard, G. Zhou, and P. Kisa (University of Pittsburgh) is gratefully acknowledged.

References

[1]Murad, E., "Spacecraft Interaction with Atmospheric Species in Low Earth Orbit," *Journal of Spacecraft and Rockets*, Vol. 33, No. 1, 1996, pp. 131–136.

[2]Rutledge, S. K., and Mihelcic, J. A., "The Effect of Atomic Oxygen on Altered and Coated Kapton Surfaces for Spacecraft Applications in Low Earth Orbit," *Materials Degradation in Low Earth Orbit (LEO)*, Minerals, Metals and Materials Society, Warrendale, PA, 1990, pp. 35–48.

[3]Rutledge, S. K., and Olle, R. M., "Space Station Freedom Solar Array Blanket Coverlay Atomic Oxygen Durability," *Proceedings of the 38th Int'l. SAMPE Symposium*, Society for the Advancement of Material and Process Engineering, Covina, CA, 1993, pp. 679–693.

[4]Brunsvold, A. L., Minton, T. K., Gouzman, I., Grossman, E., and Gonzalez, R., "An Investigation of the Resistance of Polyhedral Oligomeric Silsesquioxane Polyimide to Atomic-Oxygen Attack," *High Performance Polymers*, Vol. 16, No. 2, 2004, pp. 303–318.

[5]Banks, B., Rutledge, S., and Auer, B., "Atomic Oxygen Undercutting of Defects on SiO_2 Protected Polyamide Solar Array Blankets," *Materials Degradation in Low Earth Orbit (LEO)*, Minerals, Metals and Materials Society, Warrendale, PA, 1990, p. 15.

[6]Banks, B., Rutledge, S., de Groh, K., and Auer, B., "Atomic Oxygen Protective Coatings," *NATO Advanced Study Institute Conference*, NASA, Washington, DC, 1991.

[7]MTI Corp., URL: www.mticrystal.com [cited 1 March 2005].

[8]Eaglsham, D., Higashi, G., and Cerullo, M., "370 C Clean for Si Molecular Beam Epitaxy Using HF Dip," *Applied Physics Letters*, Vol. 59, No. 6, 1991, pp. 685–687.

[9]Nakazawa, M., Nishioka, Y., Sekiyama, H., and Kawaze, S., "Investigation of the SiO_2/Si Interface. II. Oxidation of an HF Cleaned Si(100) Surface Using Photoemission Spectroscopy with Synchrotron Radiation," *Journal of Applied Physics*, Vol. 65, No. 10, 1989, pp. 4019–4023.

[10]Thompson, P., Twigg, M., Goodbey, D., Hobart, K., and Simons, D., "Low Temperature Cleaning Processes for Si Molecular Beam Epitaxy," *Journal of Vacuum Science and Technology B*, Vol. 11, No. 3, 1993, pp. 1077–1082.

[11]Higashi, G., Becker, R., Chabel, Y., and Becker, A., "Comparison of Si(111) Surfaces Prepared Using Aqueous Solution of NH_4F Versus HF," *Applied Physics Letters*, Vol. 58, No. 15, 1991, pp. 1656–1658.

[12]Trucks, G., Raghavachari, K., Higashi, G., and Chabal, Y., "Mechanism of HF Etching of Silicon Surfaces: A Theoretical Understanding of Hydrogen Passivation," *Physical Review Letters*, Vol. 65, No. 4, 1990, pp. 504–507.

[13]Tagawa, M., Yokota, K., Ohmae, N., and Kinoshita, H., "Volume Diffusion of Atomic Oxygen in Alpha-SiO_2 Protective Coating," *High Performance Polymers*, Vol. 12, No. 1, 2000, pp. 53–63.

[14]Caledonia, G. E., Krech, R. H., and Green, B. D., "High Flux Source of Energetic Oxygen Atoms for Material Degradation Studies," *AIAA Journal*, Vol. 25, No. 1, 1987, pp. 59–63.

[15]Oakes, D. B., Krech, R. H., Upschuete, B. L., and Caledonia, G. E., "Oxidation of Polycrystalline Silver Films by Hyperthermal Oxygen Atoms," *Journal of Applied Physics*, Vol. 77, No. 5, 1995, pp. 2166–2172.

[16]Randjelovic, M., and Yang, J. C., "Structural Comparisons of Passivated Si(100) by Atomic and Molecular Oxygen," *Materials at High Temperatures*, Vol. 20, No. 3, 2003, pp. 281–285.

[17]Treacy, M. M. J., and Gibson, J. M., "Variable Coherence Microscopy: A Rich Source of Structural Information from Disordered Systems," *Acta Crystallographica Section A*, Vol. 52, No. 2, 1996, pp. 212–220.

[18]Kisa, M., Twesten, R. D., and Yang, J. C., "Structural Comparisons of SiO_x and Si/SiO_x Formed by Passivation of Single-Crystal Silicon by Atomic and Molecular Oxygen," *Materials Research Society Symposium Proceedings*, E4.7, Vol. 786, 2004, pp. 267–272.

[19]Garvie, L. A. J., and Buseck, P. R., "Bonding in Silicates: Investigation of the SiL2,3 Edge by Parallel Electron Energy-Loss Spectroscopy," *American Mineralogist*, Vol. 84, Dec. 1998, pp. 946–964.

[20]PCPDF, Personal Computer Powder Diffraction Files, Software Package, Release 1999, Data Sets 1–49 plus 70–86, International Centre for Diffraction Data, Newtown Square, PA, 1999.

[21]Kisa, M., Minton, T. K., and Yang, J. C., "Structural Comparisons of SiO_x and Si/SiO_x Formed by the Exposure of Silicon (100) to Molecular Oxygen and to Hyperthermal Atomic Oxygen," *Journal of Applied Physics*, Vol. 97, No. 2, 2005, 023520.

[22]Tagawa, M., Ema, T., Kinoshita, H., Ohmae, N., Umeno, M., and Minton, T. K., *Japanese Journal of Applied Physics*, Vol. 37, 1998, pp. L1455–L1457.

[23]Elliot, S. R., *Physics of Amorphous Materials*, 2nd ed., Longman, New York, 1983, Chap. 3.2.

[24]Voyles, P. M., Gibson, J. M., and Treacy, M. M. J., "Fluctuation Microscopy: A Probe of Atomic Correlations in Disordered Materials," *Journal of Electron Microscopy*, Vol. 49, No. 2, 2000, pp. 259–266.

[25]Voyles, P. M., and Abelson, J. R., Final Rept., National Renewable Energy Lab., Golden, CO, Oct. 2003.

[26]Tagawa, M., Yokota, K., Ohmae, N., Kinoshita, H., and Umeno, M., "Oxidation Properties of Hydrogen-Terminated Si(100) Surface Following Use of Hyperthermal Broad Atomic Oxygen Beam at Low Temperatures," *Japanese Journal of Applied Physics*, Vol. 40, Pt. 1, No. 10, 2001, pp. 6152–6156.

[27]Irene, E., "Thermionic Emission Model for the Initial Regime of Si Oxidation," *Applied Physics Letters*, Vol. 51, No. 10, 1987, pp. 767–769.

[28]Irene, E., "Thermal Oxidation of Silicon: New Experimental Results and Models," *Applied Surface Science*, Vol. 30, No. 1–4, 1987, pp. 1–16.

[29]Ichimura, S., Kurokawa, A., Nakamura, K., Itoh, H., Nonaka, H., and Koike, K., "Ultrathin SiO_2 Film Growth on Si by Highly Concentrated Ozone," *Thin Solid Films*, Vols. 377–378, Dec. 2000, pp. 518–524.

[30]Itoh, H., Nakamura, K., Kurokawa, A., and Ichimura, S., "Initial Oxidation Process by Ozone on Si(100) Investigated by Scanning Tunneling Microscopy," *Surface Science*, Vols. 482–485, Pt. 1, June 2001, pp. 114–120.

[31]Uchiyama, T., and Tsukada, M., "Scanning-Tunneling-Microscopy Images of Oxygen Adsorption on the Si(001) Surface," *Physical Review B*, Vol. 55, No. 15, 1997, pp. 9356–9359.

[32]Watanabe, H., Kato, K., Uda, T., Fujita, K., and Ichikawa, M., "Kinetics of Initial Layer-by-Layer Oxidation of Si(001) Surfaces," *Physical Review Letters*, Vol. 80, No. 2, 1998, pp. 345–348.

[33]Kuznetsova, A., Zhou, G., Chen, X., Yang, J., and Yates, J. T., Jr., "Making a Superior Oxide Corrosion Passivation Layer on Al Using Ozone," *Langmuir*, Vol. 17, No. 7, 2001, pp. 2146–2152.

D. Edwards
Associate Editor